Genomic integrity in the male germ line: evidence in support of the disposable soma hypothesis

Miguel J. Xavier[1], Lisa A. Mitchell[1], Kristen E. McEwan[1], Rodney J Scott[2], R. John Aitken[1,2] *

[1]Priority Research Centre for Reproductive Science, Faculty of Science, University of Newcastle and [2]Hunter Medical Research Institute, NSW, Australia

Running title: Disposable soma

* Corresponding author: R. John Aitken FRSE, FAA, Priority Research Centre for Reproductive Science, Discipline of Biological Sciences, Faculty of Science and IT, University of Newcastle, Callaghan NSW 2308, and Hunter Medical Research Institute, Kookaburra Circuit, New Lambton Heights, NSW 2305.

E-mail address: john.aitken@newcastle.edu.au

Abstract

The Big Blue® λ*Select-cII* selection system has been employed along with whole-exome sequencing, to examine the susceptibility of the male germ line to mutation in two challenging situations: (i) exposure to a chemotherapeutic regime including bleomycin, etoposide and *cis*-platinum (BEP) and (ii) the ageing process. A 3-week exposure to BEP induced complete azoospermia associated with a loss of developing germ cells and extensive vacuolization of Sertoli cell cytoplasm. Following cessation of treatment, spermatozoa first appeared in the caput epididymis after 6 weeks and by 12 weeks motile spermatozoa could be recovered from the cauda, although the count ($P < 0.001$) and motility ($P < 0.01$) of these cells was significantly reduced and superoxide generation was significantly elevated ($P < 0.001$). Despite this increase in free radical generation, no evidence of chromatin instability was detected in these spermatozoa. Furthermore, embryos obtained from females mated at this 12-week time point showed no evidence of an increased mutational load. Similarly progressive ageing of Big Blue® mice had no impact on the quality of the spermatozoa, fertility or mutation frequency in the offspring despite a significant increase in the mutational load carried by somatic tissues such as the liver ($P < 0.05$). We conclude that the male germ line is highly resistant to mutation in keeping with the disposable soma hypothesis, which posits that genetic integrity in the germ cells will be maintained at the expense of the soma, in light of the former's sentinel position in safeguarding the stability of the genome.

Keywords: spermatozoa; chemotherapy; ageing; mutation; embryo quality

Introduction

The 'disposable soma' hypothesis recognizes that investment in the maintenance and repair of somatic cells has to be balanced by a commitment to the germline and reproduction (Kirkwood, 1977). Thus, species that invest heavily in reproduction early in life, experience a compensatory increase in somatic senescence that directly impacts longevity. Because the germline is essentially immortal, it is critical that DNA surveillance and repair are optimized in such cells in order to keep spontaneous mutation levels to an absolute minimum and mitigate the risk of extinction (Kirkwood & Austad, 2000). Both male and female germ cells are therefore thought to be endowed with highly specialized, sophisticated mechanisms to maintain a low mutation rate, protecting the germ line at the expense of the soma (Murphey *et al*., 2013). Notwithstanding such measures, the male germ line is more vulnerable to spontaneous mutations than the female, for the simple reason that male germ cells are constantly replicating, while the female germ line spends most of its post-natal existence in a state of meiotic repose (Crow, 2000). Furthermore, the male gamete has to undertake a potentially hazardous journey between the site of insemination and the oocyte, during which the chromatin may be subjected to significant oxidative stress (Huang *et al*., 2015).

In this study, we sought to interrogate the disposable soma hypothesis by examining two paradigms in which the proposed separation of germline and somatic cell susceptibility to mutation might be tested: ageing and exposure to chemotherapeutic reagents. These studies have been undertaken employing whole exome sequencing methodologies as well as a transgenic mouse (Big Blue®), which can be used to provide objective data on mutation frequencies in multiple tissues (Nohmi *et al*., 2000). This animal model harbours multiple tandem copies of the λ*LIZ* shuttle vector randomly incorporated into its genome, and, in combination with the λ*Select-cII* system provides a quantitative measure of the mutational load carried by cells and tissues.

An analysis of the extent to which the genetic integrity of the germ line is maintained following exposure to chemotherapeutic reagents was stimulated by the rising incidence of testicular cancer, which is currently the dominant cancer of young men aged 20-34 years of age (Ziglioli *et al*., 2011). These tumours may be seminomas or non-seminomas and exhibit a peak incidence in the fourth

decade for the former and a decade earlier for the latter (Skakkebaek, 1972; Reuter, 2005; Looijenga *et al*., 2011). For reasons that are still unclear, the incidence of testicular germ cell tumours, while low, has been increasing in recent decades, possibly as a result of fetal exposure to environmental factors such as phthalate esters polychlorinated biphenyls or polyvinyl chlorides during pregnancy (Meeks *et al*., 2012).

The treatment options for testicular cancer may involve combinations of surgery, radiation and chemotherapy depending on the location and type of cancer and its degree of progression (Shelley *et al*., 2002; Mortensen *et al.,* 2011). Such treatments are very successful, generating extremely high 5-year survival rates that approach 100% for both types of germ cell tumour (van Basten *et al.,* 1997; Stang *et al*., 2013). The available clinical and animal data suggest that the major form of chemotherapy used in the treatment of testicular cancer, comprising a mixture of bleomycin, etoposide and cisplatin (the BEP regime), very effectively suppresses spermatogenesis without destroying the spermatogonial stem cell population (Sweeney, 2001; Marcon *et al.,* 2008). As a result, spermatogenesis is known to return following BEP treatment, as is fertility (Marcon *et al.,* 2008). However questions remain concerning the absolute normality of the spermatozoa generated following exposure to BEP as well as the health trajectory of any progeny (Maselli *et al*., 2012). Thus in rats, the return of fertility after BEP treatment is associated with an increase in preimplantation embryonic loss, which the authors attribute to an effect on the spermatogonia (Marcon *et al*., 2008). By contrast, clinical studies have generally failed to find evidence for an increased risk of congenital malformations in the offspring of males who have previously been exposed to alkylating reagents in the course of their cancer treatment (Chow *et al*., 2009; Signorello *et al*., 2012). Against this background, a slight increase in the relative risk of congenital birth abnormalities (RR=1.17) was detected by Stahl *et al*. (2011) in the offspring of men with a history of cancer. Given such uncertainty in the literature, Choy & Brannigan (2013) have called for additional research that will allow for the development of clinical guidelines to assist cancer patients, considering post-treatment conception, in their decision-making processes.

The second scenario where investment in the maintenance of genetic integrity in the germ line might be called into question is ageing. The latter results from the progressive accumulation of

somatic damage as a consequence of limited investment in maintenance and restoration at the cellular level, particularly with respect to DNA repair and antioxidant protection pathways (Kirkwood & Austad, 2000). The extent to which the male germ line is protected from the impact of ageing is controversial since there is ample evidence to suggest that ageing does induce high level of oxidative stress and DNA damage in male germ cells (Smith *et al.,* 2013; Selvaratnam & Robaire, 2016) even though other evidence suggests that the germ line is relatively protected from the processes driving senescence (Hill *et al*., 2004; Murphey *et al*., 2013).

In light of the above considerations, we have used the Big Blue® model and whole–exome sequencing to quantify the vulnerability of the male germ line to mutate in the wake of two potentially mutagenic stimuli, chemotherapy and advancing age.

Materials and methods

Chemicals and Reagents

Unless otherwise stated, all chemicals and reagents were obtained from Sigma-Aldrich (St Louis, MO, USA) while fluorescent probes were obtained from Molecular Probes (Eugene, OR, USA).

Animal treatment and embryo collection

All experimental procedures were conducted with the approval of the University of Newcastle's Animal Care and Ethics Committee. Big Blue® transgenic rodents (Agilent, Santa Clara, CA, USA) homozygous for the λLIZ shuttle vector were obtained from Australian BioResources Ltd (Moss Vale, NSW, Australia). Adult males treated with chemotherapy were subjected to a BEP (Bleomycin, Etoposide, Platinum agent) regime commencing when males were between 2-4 months of age and extending for 3 weeks. Mice receiving BEP treatment received etoposide (5mg/kg, Pfizer, New York, NY, USA) and cisplatin (1 mg/kg, Sigma) in 0.9% saline via IP injection on days 1, 3-5 of each week, and etoposide, cisplatin and bleomycin (828 IU/kg, Hospira Lake Forest, IL, USA) via IP injection on day 2 of each week. Control mice received 0.9% saline via IP injection on days 1-5 of each week. Following the 3-week treatment period, males were allowed to recover for up to 24 weeks. Big Blue®

females were then used for natural matings at 12, 16 and 24 weeks post treatment in order to assess the long-term impact of BEP exposure on fertility in vivo. The foetuses generated from the 12-week matings were used for mutation analysis. For this purpose, viable embryos were collected at 14 days *post coitum* (dpc), snap-frozen in liquid nitrogen and stored at −80°C. For the 12-week time point, there were 16-31 mice per group. Testis weight, sperm motility and cell counts were conducted on 15-31 mice, while for all other assays, a minimum of 3 mice were used. For all other time points, 3-7 mice were analysed. For mating studies, 2-5 pairings were conducted for each time point.

For the ageing study liver, testis and spermatozoa were collected from Big Blue® male mice at 2-4, 9-11, 17-20 and 21-23 months of age. For the mating studies, males from these three age groups were mated to females 1-3 (young) or 8-10 months (old) of age (corresponding to advanced middle age but still capable of generating offspring). Embryos from these matings were collected 14 days dpc, snap-frozen in liquid nitrogen and stored at -80°C. For these studies, 19-22 male mice were analysed per age group. Testis weight and sperm motility were conducted on 16-22 mice per group, while all other assays were conducted on 3-10 mice per group. For mating studies, 4-10 pairings were conducted for each age group.

Collection of spermatozoa and tissue

Mice were euthanized via carbon dioxide asphyxiation and spermatozoa and testes were collected immediately. Caudal epididymal spermatozoa were collected by back-flushing and deposition of the perfusate under oil at 37°C. The sperm population was then diluted in 1ml modified Biggers, Whitten, and Whittingham medium (BWW) (Biggers *et al.*, 1971) supplemented with 0.1% PVA, 0.27 mM sodium pyruvate, 44 mM sodium lactate, 5 U/ml penicillin, 5 mg/ml streptomycin and 20 mM HEPES buffer. Caput spermatozoa were obtained via gentle dissection of the tissue in 1 ml BWW followed by filtration through a 70 μm nylon mesh strainer. Testes were fixed overnight in Bouin's solution and washed 3x in 70% ethanol before being embedded in paraffin, sectioned and stained with haemotoxylin and eosin. Testicular sections were subsequently examined to determine the

131 percentage of tubular cross sections exhibiting evidence of impaired spermatogenesis as described by
132 Marcon *et al.* (2008). Two tissue sections were analysed per testis, from 3-4 animals per time point.
133 One hundred tubular cross sections were analysed per slide and thus 200 tubular cross sections in
134 total analysed per animal. Tubules were classified as exhibiting disrupted spermatogenesis when there
135 was extensive vacuolisation of the Sertoli cells, disorganisation of the germ cells, or a lack of later
136 germ cell types (eg. beyond spermatogonia or, sometimes, spermatocytes) present.
137
138 ***Computer Assisted Sperm Analysis***
139 Caudal epididymal sperm motility was assessed with a Hamilton Thorne CASA System Version 12
140 IVOS (Hamilton Thorne Biosciences, Beverly, MA, USA). Motility was scored for at least 200 cells
141 per sample. Motility was defined as an average path velocity greater than 5 μm/s while progressive
142 motility was defined as an average path velocity greater than 25 μm/s and a straightness value greater
143 than 80%. The image acquisition settings were: negative phase-contrast optics; recording rate 60
144 frames/sec; minimum contrast 80; minimum cell size 3 pixels; low size gate 1.0; high size gate 2.9; low
145 intensity gate 0.6; high intensity gate 1.4; non-motile head size 6 and non-motile head intensity 160.
146
147 ***MitoSOX Red (MSR) and Dihydroethidium (DHE) Assays***
148 To determine the generation of mitochondrial or overall cellular superoxide anion, MitoSOX Red or
149 dihydroethidium was used respectively (Aitken *et al.*, 2013). These probes were added to cells at a
150 final concentration of 2 μM, accompanied by the viability stain, SYTOX Green, at a final concentration
151 of 0.05 μM. Following 15 min incubation at 37°C, the spermatozoa were centrifuged for 3 min at 600
152 *g* before being resuspended in 300 μl BWW. Fluorescence was then measured on a FACSCalibur
153 flow cytometer with CellQuest Pro software (Becton Dickinson, San Diego, CA, USA). Argon laser
154 excitation at 488 nm was coupled with emission measurements using 530/30 band pass (green) and
155 585/42 band pass (red) filters. A total of 10,000 events were recorded following gating out of non-
156 spermatozoa-specific events.
157

JC-1 assay

To measure mitochondrial membrane potential, JC-1 probe was added to cells at a final concentration of 6.25 µM. Following 15 min incubation at 37°C, the spermatozoa were centrifuged for 3 min at 600 *g* before being resuspended in 400 µl BWW. Just prior to analysis, propidium iodide was added to each sample at 10 µg/ml. Fluorescence was then measured on a FACSCalibur flow cytometer with CellQuest Pro software (Becton Dickinson, San Diego, CA, USA). Argon laser excitation at 488 nm was coupled with emission measurements using >670 long pass filter (far red; propidium iodide) to exclude dead cells from analysis, followed by 530/30 band pass (green; low MMP) and 585/42 band pass (red; High MMP) filters. A total of 10,000 events were recorded following gating out of non-spermatozoa-specific events.

8-hydroxy-2'-deoxyguanosine (8OHdG)

Snap-frozen spermatozoa samples were thawed and incubated overnight at 4°C in 25 µg/ml DNA/RNA Damage Antibody (Novus Biologicals, Littleton, CO, USA) in phosphate-buffered saline containing 0.1% Tween (PBST). Cells were washed with phosphate-buffered saline (PBS), incubated with Alexa Fluor 488 antibody (ThermoFisher, Waltham, MA, USA) in PBST for 1 h at room temperature and then washed twice with PBS. Cells were mounted on slides and counted on a fluorescent Zeiss Axio Imager A.1 (Carl Zeiss GmbH, Oberkochen, Germany). A total of 100 cells was counted for each sample.

Sperm Chromatin Structure Assay (SCSA)

Following isolation, spermatozoa were washed with BWW, snap-frozen in liquid nitrogen and stored at −80°C. SCSA was performed as described by Evenson & Jost (2000) using a FACScan Flow Cytometer with CellQuest software (Becton Dickinson, San Diego, CA, USA). Briefly, 200 µl acid detergent solution (0.08 N HCl, 0.1 5M NaCl, 0.1% Triton X-100, pH 1.2) was added to thawed cells. Following a 30 s incubation, 600 µl acridine orange staining solution was added and the sample was run through the flow cytometer for 2.5 min before acquisition. A total of 5,000 events were recorded

following gating out of debris. Cells in the main population and those with high DNA stainability, representing immature spermatozoa, were subtracted from the total number of cells analysed to calculate %COMP, the proportion of cells outside the main population with abnormal chromatin structure.

DNA extraction for λSelect-cII Mutation Detection assay and whole-exome sequencing

High molecular weight genomic DNA was extracted from adult testes, livers and 14 dpc whole embryos using the RecoverEase DNA Isolation Kit (Agilent, Santa Clara, CA, USA) according to the manufacturer's protocol with the following modifications. A 2 ml Kontes dounce tissue grinder (Kimble Chase, Rockwood, TN, USA) was used to homogenise each embryo in 1 ml lysis buffer. Pestle B was used for 10-12 strokes to homogenise each sample. After pouring each sample through the cell strainer, a further 7 ml of lysis buffer was used to wash the tissue grinder to bring the total sample volume to 8 ml. Following addition of digestion solution, 70 µl of warm proteinase K solution (2 mg/ml proteinase K, 2% SDS, 0.1 M EDTA) was added before each sample was incubated at 50°C for 45 min. Following this incubation, the sample was dialysed against TE Buffer (10 mM Tris-HCl pH 7.5, 1 mM EDTA) for 24-72 h, as required. On completion of dialysis the fully hydrated genomic DNA was recovered and stored at 4°C.

Determination of cII mutant frequency

The λLIZ shuttle vector was packaged using Transpack Packaging Extract (Agilent, Santa Clara, CA, USA) according to the manufacturer's protocol, with several modifications. Briefly, following the final 90 min incubation, 1.1 ml SM buffer (100 mM NaCl, 8 mM $MgSO_4.7H_2O$, 50 mM Tris-HCl pH 7.5, 0.01% w/v gelatin) were added to each sample as described in the *λ Select-cII* Mutation Detection System for Big Blue® Rodents protocol (Agilent, Santa Clara, CA, USA). Titering and screening then proceeded as described in the *λ Select-cII* protocol using G1250 *E. coli* cells on TB1 agar (1.2% bacto agar, 1% bacto-tryptone, 0.5% NaCl, 0.0001% thiamine hydrochloride). Ultimately, *cII*− mutants were measured by growing infected G1250 bacteria on TB1 plates at 24°C for approximately 46 h. During

this incubation, infections involving phage with a wild-type *cII* gene undergo lysogenization (a process by which bacteria acquire phage sequences that become integrated into their genome) and the infected bacteria become part of the developing lawn, while phage with a mutated *cII* gene undergo a lytic cycle, giving rise to plaques. At 37°C, all phage undergo the lytic cycle and form plaques regardless of whether they are carrying a wild-type or mutant *cII* gene, enabling titering of the total plaque forming units (pfu) screened. The *cII* mutant frequency was calculated as the number of mutant plaques per total plaques screened.

Determination of cII mutation frequency

The *cII* sequence from every successfully replated mutant was sequenced following PCR amplification and purification as follows: 5 µl sample was combined with 2.5 mM $MgCl_2$, 1 x reaction buffer, 0.5 mM each dNTP, 1 µM each primer (upstream: 5'-CCGCTCTTACACATTCCAGC-3', downstream: 5'-CCTCTGCCGAAGTTGAGTAT-3') and either 2.5 U or 1 U Taq (Taq2000 DNA Polymerase, Agilent, Santa Clara, CA, USA or Taq DNA Polymerase Native, Invitrogen, Grand Island, NY, USA, respectively) in a total reaction volume of 20 µl. A 476 bp amplicon was produced in an Eppendorf Mastercycler (Eppendorf, Hamburg, Germany) with the following cycling conditions: an initial 3 min denaturation step at 95°C, 35 cycles of denaturation at 95°C for 30 sec, annealing at 62°C for 1 min and extension at 72°C for 1 min, followed by a final extension at 72°C for 10 min. Amplicons were purified using the Wizard SV Gel and PCR Clean-Up System (Promega, Madison, WI, USA) and ethanol precipitated before being sequenced. The PCR primers detailed were also used as sequencing primers. Mutations were identified using NCBI Nucleotide BLAST, FinchTV Version 1.4 software (Geospiza, Seattle, WA, USA) and the published wild-type lambda sequence (Accession #J02459). When this analysis did not identify a mutation, PCR and sequencing were repeated using a second upstream primer to cover the PR promoter region (5'-GCGACAGATTCCTGGGATAA-3'), however this strategy did not reveal any additional mutations in the promoter region. When the same mutation was found multiple times in one sample it was assumed to be a jackpot mutation and was therefore counted as a single independent mutation. When a mutant exhibited multiple types of

mutations, these mutations were scored as a single complex mutation. The mutation frequency was then calculated as the number of independent mutations per total plaques screened.

Calculation of the mutational load present in exome of embryos

The genomic DNA extracted from embryos conceived by young and old parents were prepared for whole-exome sequencing. In the young group, males and females were 2-4 and 1-3 months of age respectively, while in the aged group, the corresponding figures were 17-20 and 8-10 months of age respectively; n = 4 for all analyses. Samples containing approximately 100 µg/mL of genomic DNA were placed in a Covaris Sonicator (Covaris, Woburn, MA, USA) to generate 150-200 bp DNA fragments. Each sample was treated with SureSelectXT Target Enrichment System for Illumina Paired-End Sequencing Library (Agilent, Santa Clara, CA, USA) and sequencing was performed on a Mi-Seq Sequencer (Illumina, San Diego, CA, USA). Raw sequence reads obtained by sequencing were imported into and analysed with the NextGENe Software (SoftGenetics, State College, PA, USA). Sequence reads were mapped against the NCBI and Mouse Genome Sequence Consortium Build 37 (NCBI37/mm9) (July 2007, NCBI). Mutations detected on genes with coverage lower than 15 reads and calling scores below 12 were considered to be alignment or base-calling errors, and were excluded from further analysis. Mutational load in each sequenced sample was calculated from validated mutations per nucleotide and averaged for comparison between mating groups. Mutations identified as matching common known single nucleotide polymorphisms (SNPs) present in the dbSNP database (Sherry *et al.* 2001) were excluded from the calculation of *de novo* mutation rate. Mutations present in at least 90% of all the samples were considered established mutations in the mouse strain and also excluded from the calculations.

Statistical analysis

All experiments were replicated at least 3 x on independent samples and the results analyzed by one- and two- way ANOVA using the SuperANOVA program (Abacus Concepts Inc, CA, USA) on a MacIntosh G4 Powerbook computer; post hoc comparison of group means was by Fisher's PLSD

(Protected Least Significant Difference). Mutation spectra were analysed using the Cariello *et al.* (1994) program. For the exome analysis, all experimental results obtained were imported into R Statistical Software (R Core Team 2004). Differences in mutation frequency were determined by performing the Mann-Whitney U test in light of the data's non-parametric distribution. Paired comparisons of litter sizes and embryonic resorptions per successful mating of young and aged parents were also calculated using the Mann-Whitney U tests. A Kruskal-Wallis one-way analysis of variance and the post-hoc multiple comparison test, kruskalmc test in R, was performed to compare mutational frequencies in tissue samples.

Results

Chemotherapy

Testicular histology

One week after cessation of the 3-week treatment period, the histology of the testes revealed a profound disruption of spermatogenesis in the BEP-treated animals, in contrast to the vehicle-only controls (Fig. 1). In the treated animals, a majority of the tubules were devoid of differentiating germ cells and instead presented with highly vacuolated Sertoli cells and exfoliated immature germ cells in the tubule lumina. Around the periphery of the seminiferous tubules, a single layer of spermatogonia remained bound to the basement membrane and still appeared to be viable. Similarly, the interstitial tissue did not appear to have been dramatically affected by temporary exposure to BEP (Fig. 1). During the ensuing 20 weeks spermatogenesis gradually recovered, with fewer and fewer tubular cross sections showing evidence of severely disrupted spermatogenesis (Fig. 1, 2A). Nevertheless even 24 weeks after the cessation of BEP treatment, occasional tubules could be found that still exhibited vacuolated Sertoli cell cytoplasm and a complete absence of germ cell development (Fig. 1, 2A). The long-lasting effects of BEP treatment were also evident from the testicular weights which, though improved, had still not returned to control levels after 24 weeks of recovery (Fig. 2B). Despite such lingering effects of BEP exposure, it should be noted that litter sizes were not significantly different between control and BEP-exposed fathers 12, 16 and 24 weeks after treatment (Fig. 2C).

293 Similarly, the number of embryonic resorption sites was not significantly different between control
294 and treated animals at these time points (Fig. 2D).
295
296 ***Sperm quality***
297 1 week after the cessation of treatment there were very few spermatozoa in the caput epididymis,
298 indicating that sperm production had been severely compromised by BEP exposure ($P < 0.001$; Fig.
299 3A). Spermatozoa were present in low numbers at 6 and 12 weeks and afterwards numbers increased
300 but remained significantly ($P < 0.001$) below control levels as long as 24 weeks the cessation of
301 treatment (Fig. 3A). Some residual spermatozoa were recovered from the cauda epididymis 1 week
302 after the cessation of treatment (Fig. 3B) but by 6 weeks had declined to negligible levels reflecting
303 the severe disruption of spermatogenesis ($P < 0.001$). Even by the 12th post-treatment week, the
304 numbers of spermatozoa stored in the cauda epididymis were still low and remained significantly
305 below control values 24 weeks after the cessation of treatment ($P < 0.01$; Fig. 3B). The few
306 spermatozoa recovered 6 weeks after the cessation of treatment were all immotile (Fig. 3C,D); by
307 the 12th week, both motility and progressive motility were clearly improving, although these quality
308 measures were still significantly below control levels at this time point ($P < 0.01$ and $P < 0001$
309 respectively). However, by the 16th week, neither motility nor progressive motility were significantly
310 different from the controls. An analysis of reactive oxygen species (ROS) generation by the
311 spermatozoa revealed a significant increase in the generation of mitochondrial ROS as early as 1 week
312 post treatment ($P < 0.05$), which then remained elevated until the 24th week ($P < 0.01$; Fig. 3E).
313 Cytoplasmic superoxide generation as measured by DHE oxidation was also significantly elevated 12
314 weeks post-treatment ($P < 0.01$) but then returned to control levels by the 16th week (Fig. 3F).
315 These results indicated that by 12 weeks after the cessation of BEP treatment, small numbers
316 of spermatozoa were appearing in the epididymis with significantly reduced total motility levels
317 accompanied by high levels of ROS generation. In order to determine whether the oxidative stress
318 observed in the spermatozoa during this recovery phase influenced DNA integrity in these cells, a
319 SCSA analysis was performed (Fig. 4A,B). According to this assay, no significant induction of DNA

damage was evident at any time during the 24-week recovery period (Fig. 4B). At all time intervals tested the %COMP values recorded in the SCSA assay were low and not significantly different from the control animals (Fig. 4B). As a positive control for this assay, we also examined caput epididymal spermatozoa, which are known to generate high SCSA values (Pérez-Cerezales *et al*., 2012). This is because the chromatin of caput epididymal cells is still not fully stabilized by disulphide bond formation and, as a result, exhibits an enhanced susceptibility to the acid denaturation conditions employed in the SCSA system (Bennetts & Aitken, 2005). As anticipated, immature spermatozoa from the caput epididymis exhibited significantly higher SCSA signals compared with caudal cells ($P < 0.001$) but at no time point did caput spermatozoa from BEP–exposed animals generate higher SCSA signals than their unexposed controls (Fig. 4A).

Mutation assays following chemotherapy and ageing

Examination of testicular tissue from mice sampled 12 weeks after BEP treatment revealed a significant increase in mean mutation frequency relative to the controls ($P = 0.036$; Table 1) in the absence of any particular change in the spectrum of independent mutations observed (Table 2). In order to determine whether these mutations were in the somatic or germ cell component of the testes the mean mutant frequency, describing the fraction of λ*LIZ* shuttle vectors carrying mutations in the *cII* gene, was examined in spermatozoa and found to be identical ($3.1 \pm 1.0 \times 10^5$ vs $3.1 \pm 1.0 \times 10^5$ in BEP-treated and control groups respectively, with 2,640,668 plaques screened). A subsequent analysis of mutation frequencies in day 14 embryos generated from BEP-treated and control males mated to untreated females revealed no increase in mutation frequency as a consequence of chemotherapeutic exposure ($2.9 \pm 0.2 \times 10^5$ vs $2.7 \pm 0.3 \times 10^5$; Table 3). In Table 4 the types of independent mutations recorded in these two groups of animals is presented. In both the control and BEP-exposed groups the predominant type of mutation was a G to A transition followed by G to T transversions. Analysis of the mutation spectra between the two groups did however reveal a significant difference ($P < 0.05$), with the offspring of chemotherapy-treated males notably exhibiting fewer C to T transitions and more G to T transversions than the controls (Table 4).

Ageing of either males (or their female partners) also had no significant impact on the mutation frequencies seen in day 14 embryos (Table 5) or the spectra of independent mutations observed (data not shown). The whole-exome analysis of embryos conceived from differentially aged parents generated data for 203,225 exonic regions of the mouse genome, collectively comprising 4.54 × 10^{-8} bases per sample with an average coverage of 10 per base. The absolute number of *de novo* mutations in the exomes of the offspring of young or aged parents was found to be not statistically different (Fig. 5A) comprising 1352.0 ± 19.8 and 1356.5 ± 8.8 mutations per individual for matings involving young and old progenitors respectively. Overall, the type of mutation found in the genome of the offspring of young and aged mice, was predominantly base substitutions with a transition/transversion ratio of 1.05.

The mutation frequency obtained from sequencing the whole-exome of the offspring of young and aged parents was also determined to be not statistically different (Fig. 5B). The mutation frequency observed in the offspring resulting from the mating of young or old mice was 2.98 × 10^{-7} ± 4.36 × 10^{-9} and 2.99 × 10^{-7} ± 1.95 × 10^{-9} mutations per base pair (bp), respectively. The overall mutation frequency carried in the exome of embryos conceived by both groups was calculated to be 2.98 × 10^{-7} ± 2.40 × 10^{-9} mutations per bp.

These data suggested that the male germ line is protected from the impact of ageing in this strain of mouse in contrast to somatic tissues such as the liver where a significant increase ($P < 0.05$) in mutation frequency was observed with age (Table 6). The concept that the germ line of Big Blue® mice is protected from age-dependent deterioration was also consistent with the analysis of male reproductive function during ageing in this strain (Fig. 5). Thus, age was found to have no significant impact on testes weight (Fig. 5C), sperm motility (Fig. 5D), sperm DNA damage (Fig. 5E) or 8OHdG formation (Fig. 5F). Significantly elevated levels of DNA fragmentation were observed in caput vs caudal epididymal spermatozoa ($P < 0,001$; Fig 5E) reflecting the differences in DNA compaction in these two populations of spermatozoa, however this change was not influenced by age. Interestingly, mitochondrial superoxide generation by caudal epididymal spermatozoa was found to significantly decline during epididymal maturation ($P < 0.001$; Fig. 5G) in concert with a significant increase in

mitochondrial membrane potential ($P < 0.001$; Fig. 5H), suggesting that the efficiency of mitochondrial electron transport improves as a consequence of epididymal passage. Importantly however, this biomarker of epididymal function showed no deterioration as a consequence of age (Fig. 5G,H).

Discussion

One of the key tenets of the disposable soma hypothesis is that energy will be invested in maintaining the genetic integrity of the germ line at the expense of the soma, which is more vulnerable to ageing as a consequence. We have used whole–exome sequencing and the Big Blue® transgenic mouse to examine this concept in two situations: the administration of chemotherapeutic agents and ageing.

In terms of chemotherapy, this study has confirmed the devastating effect that chemotherapeutic agents such as bleomycin, etoposide and cisplatin can have on spermatogenesis (Bieber *et al*., 2006; Delbes *et al*., 2007; Maselli *et al*., 2012). After a 3-week course of treatment, spermatogenesis was severely impaired with significant exfoliation of developing precursor germ cells in the lumen of the seminiferous tubules and extensive vacuolization of the Sertoli cell cytoplasm. As long as 12 weeks after a course of BEP treatment evidence of disrupted spermatogenesis was still evident, testis weights were still reduced, sperm numbers were still low in the caput and cauda epididymis and the spermatozoa were actively generating ROS. At this point in the recovery pathway however, sperm motility was beginning to reappear, the animals were fully fertile and we could find no evidence of DNA damage in the spermatozoa or enhanced mutation rates in the offspring. Litter sizes were also not statistically different between treated animals and controls and the offspring showed no gross morphological abnormalities. However, more subtle changes that might have been detected by weighing the pups or conducting detained autopsies, cannot be excluded. Nevertheless, at face value, these results suggest that as the germinal epithelium recovers from BEP exposure and spermatogenesis resumes, the spermatozoa that are produced are normal and fully capable of fertilization, even if they are surrounded by dysfunctional spermatozoa generated by regions of the seminiferous tubule that are still in the process of recovery.

Studies in the rat have emphasized the importance of germ cell apoptosis in BEP-induced azoospermia and have also suggested that recovery of the spermatogenic process may be impaired following exposure, with BEP-treated animals exhibiting abnormal chromatin stability according to SCSA, TUNEL and Comet assays (Delbes *et al.,* 2007). However, when BEP-treated animals were left for a further period of recovery, all evidence of DNA fragmentation receded (Maselli *et al*., 2012), although long term changes to sperm chromatin composition was suggested by high chromomycin A3 stainability, indicative of poor protamination, and a concomitant increase in the levels of histone expression (Maselli *et al*., 2012). Such data suggest a long-lasting impact of BEP exposure on the chromatin structure of mammalian spermatozoa. The histone enrichment observed under these circumstances may be an adaptive change designed to place an increased number of genes in a non-protaminated 'poised' state, ready for early, facilitated expression in the embryo (Hammoud *et al*., 2009). Alternatively, such poor protamination may place the germ line at risk by facilitating the onset of DNA damage. A large number of studies have demonstrated that poor chromatin compaction is positively correlated with a susceptibility to sperm DNA damage (Sakkas et al., 1998; Nili et al., 2009; De Iuliis et al., 2009; Castillo et al., 2011; Manochantr et al., 2012). Such observations have important implications for young male cancer survivors wishing to establish a family because DNA damage in spermatozoa has been associated with a wide range of diseases in the offspring including brain disorders such as autism, bipolar disease, spontaneous schizophrenia and epilepsy, as well as childhood cancer (Aitken & De Iuliis, 2007).

The SCSA assay is one of the most sensitive assays of DNA damage that can readily discriminate the vulnerability of poorly compacted spermatozoa in the caput epididymis from their compacted caudal epididymal counterparts and with an efficiency that is beyond the conventional TUNEL assay (Pérez-Cerezales et al., 2012l). Within our data set we found exactly the same high sensitivity to DNA damage in caput epididymal spermatozoa when the latter were exposed to the acid DNA denaturation conditions characteristic of SCSA (Fig. 4; Evenson and Jost, 2000). This sensitivity is thought to be due to the limited degree of chromatin stabilization observed in immature caput epididymal spermatozoa as a consequence of the incomplete formation of inter- and intra-

427 molecular disulphide bridges between, and within, sperm protamines (Pérez-Cerezales et al., 2012).
428 By the time epididymal maturation has been completed and these disulphide brides have been created,
429 the chromatin is in a highly stable, compacted state and in this mature condition is relatively resistant
430 to DNA damage, whether this is via an oxidative attack (Sawyer *et al*., 2003) or acid-induced
431 denaturation in the SCSA assay. The fact that the anticipated decline in SCSA reactivity as
432 spermatozoa matured in the epididymis was observed with equal facility in both our control animals
433 and our BEP-exposed males, suggests that chromatin compaction was occurring normally in the latter.
434 The spermatozoa recovered from the cauda epididymis 12-24 weeks after the cessation of BEP
435 therapy therefore showed no signs of spontaneous DNA damage nor any susceptibility to the
436 induction of such damage under denaturing conditions. Nevertheless, more subtle changes in sperm
437 chromatin integrity and structure that remain undetected by the SCSA assay, cannot be excluded.

438 These accord with the outcome of the Big Blue® mutation assay, which failed to find
439 any evidence of an increase in the mutational load carried by the offspring of BEP-exposed fathers.
440 They also accord with a growing volume of clinical data suggesting that there is no major increase in
441 the incidence of congenital birth defects in the offspring of fathers who have previously been exposed
442 to alkylating agents in the course of cancer treatment (Dohle *et al.,* 2010). While evidence does exist
443 in the rat model for impacts of paternal chemotherapy with reagents such as cyclophosphamide (Hales
444 *et al.,* 2005), these concerns were not borne out in the present animal model as far as BEP is
445 concerned. It is possible that more stringent dosing regimes may have generated a different outcome,
446 however the chemotherapeutic protocol employed in this study was clearly competent to completely
447 suppress spermatogenesis. The power of the Big Blue® model is that it permits a quantitative
448 approach to genotoxicity that can be backed up by the rigour of sequencing every single mutant
449 plaque, in order to confirm the existence of *de novo* mutations. These quantitative data serve to
450 emphasize the remarkable capacity of the spermatogonial stem cell population to not only withstand
451 chemotherapeutic attack, but also to recover from such an insult by reinitiating spermatogenesis in a
452 manner that may be quantitively impaired but maintains a high level of genetic fidelity in the
453 spermatozoa. Thus, while there was clear evidence of an increase in mutation rate within the testes

following BEP exposure (Table 1), there was no evidence of an increase in the mutational load carried in the germ line, suggesting that the increase must have been due the somatic cell constituents of this organ (for example, Sertoli or Leydig cells). Of course, it is always possible that whole genome sequencing might have revealed damage outside of the exomic regions. However, it should also be acknowledged that the Big Blue cassette inserts itself into random regions of the genome and yet we still did not see a significant increase in mutation frequency following treatment with BEP.

The only subtle change observed as a consequence of BEP-exposure was an increase in G-T transversions at the expense of C-T transitions (Table 4). The impact of such a change on the health trajectory of the offspring is difficult to ascertain. However, it may be significant that transversions, rather than transitions, have been found to have a greater impact on gene expression and have been associated with the early onset of cancer and other genetic diseases (Leonard *et al.* 2013; Lyons & Lauring, 2017; Zhan *et al.* 2017).

Analysis of the impact of paternal ageing on the mutational load carried by the progeny generated very similar results. While mutation rates significantly increased in the liver as a consequence of ageing, there was no evidence of any corresponding change in the germ line. The offspring of old fathers exhibited exactly the same mutation rate as the offspring of young fathers and the relative age of the mother did not seem to contribute to the overall levels of mutation observed. Furthermore we could see no change in the quality of the spermatozoa with age. As with the BEP study, we noted a change in the susceptibility of chromatin to the acid conditions associated with the SCSA assay as a consequence of epididymal maturation (Fig. 5E); however, this stabilization process was unaffected by age (Fig. 5E). Similarly, we noted that the mitochondria acquire functionality as a consequence of epididymal maturation, reducing the leakage of electrons to oxygen to generate superoxide anion and increasing the competence of these organelles to generate a potential difference across the inner mitochondrial membrane (Fig. 5G,H). This attribute of epididymal function did not change with paternal age.

Thus, for this strain of mouse, there is a clear preferential investment in the maintenance of the germ line with increasing age, as would have been predicted by the disposable soma hypothesis

and adding weight to the general evolutionary significance of this concept. In contrast, humankind clearly places limits on any investment in the germ line since there is incontrovertible evidence indicating that paternal ageing is associated with a loss of human fertility, elevated rates of miscarriage and an increase in the mutational load carried by the offspring (Kong *et al*., 2012; Aitken, 2013a; Johnson *et al*., 2015; Jónsson *et al*., 2017; Kaarouch *et al*., 2018). Thus, the human condition may represent a departure from the disposable soma hypothesis, with its implied high level of investment in the maintenance of the germ line. The elevated levels of infertility observed in our own species as well as the abundant evidence for paternal-age impacts on a complex sweep of conditions including achondroplasia, autism and spontaneous schizophrenia, raise fundamental questions about our species' commitment to its germ line and the validity of mouse models to study the impact of intrinsic and extrinsic factors on germ cell integrity (Aitken *et al*., 2013b; Yatsenko & Turek, 2018). The evolutionary advantage associated with such a reckless dereliction of duty in a human context may suggest the existence of a trade-off that places increased emphasis on the role of the germ line in creating genetic diversity and our resultant ability to adapt to environmental change.

Declaration of interest

The authors declare that there is no conflict of interest that could be perceived as prejudicing the impartiality of the research reported.

Funding

This study was funded by a Discovery grant from the Australian Research Council (# DP110103951).

Acknowledgements

We are extremely grateful to Dr Jennette Sakoff for supplying the chemotherapeutic drugs and to the staff of the Animal Services Unit, University of Newcastle, for their assistance with animal care and maintenance. We are also grateful to Tegan Smith for helpful discussions in relation this project

507 and the Analytical and Biomolecular Research Facility (ABRF) of the University of Newcastle for
508 access to its flow cytometry core.

509

510 **References**

511 **Aitken RJ** (2013a) Human spermatozoa: revelations on the road to conception. *F1000 Prime Reports*
512 **5**, 39.

513 **Aitken RJ** (2013b) Age, the environment and our reproductive future: bonking baby boomers and
514 the future of sex. *Reproduction* **147**, S1-S11.

515 **Aitken RJ & De Iuliis GN** 2007. Origins and consequences of DNA damage in male germ cells.
516 *Reproductive Biomedicine Online* **14**, 727-733.

517 **Aitken RJ, Smith TB, Lord T, Kuczera L, Koppers AJ, Naumovski N, Connaughton H,**
518 **Baker MA & De Iuliis GN** 2013 On methods for the detection of reactive oxygen species
519 generation by human spermatozoa: analysis of the cellular responses to catechol oestrogen, lipid
520 aldehyde, menadione and arachidonic acid. *Andrology* **1**, 192-205.

521 **Aitken RJ, Whiting S, De Iuliis GN, McClymont S, Mitchell LA & Baker MA** 2012
522 Electrophilic aldehydes generated by sperm metabolism activate mitochondrial reactive oxygen
523 species generation and apoptosis by targeting succinate dehydrogenase. *Journal of Biological*
524 *Chemistry* **287**, 33048-33060.

525 **Bennetts LE & Aitken RJ** 2005 A comparative study of oxidative DNA damage in mammalian
526 spermatozoa. *Molecular Reproduction and Development* **71**, 77-87.

527 **Bieber AM, Marcon L, Hales BF & Robaire B.** 2006 Effects of chemotherapeutic agents for
528 testicular cancer on the male rat reproductive system, spermatozoa, and fertility. *Journal of*
529 *Andrology* **27**, 189-200.

530 **Biggers JD, Whitten WK & Whittingham DG** 1971 The culture of mouse embryos in vitro, in:
531 Daniel, J.C. (Ed.), Methods in Mammalian Embryology. Freeman, SanFrancisco, pp. 86–116.

532 **Cariello NF, Piegorsch WW, Adams WT & Skopek TR** 1994 Computer program for the
533 analysis of mutational spectra: application to p53 mutants. *Carcinogenesis* **15**, 2281-2285.

534 **Castillo J, Simon L, de Mateo S, Lewis, S & Oliva R** 2011 Protamine/DNA ratios and DNA
535 damage in native and density gradient centrifuged sperm from infertile patients. *Journal of Andrology*
536 **32**, 324-332.

537 **Chow EJ, Kamineni A, Daling JR, Fraser A, Wiggins CL, Mineau GP, Hamre MR,**
538 **Severson RK, Drews-Botsch C & Mueller BA** 2009 Reproductive outcomes in male
539 childhood cancer survivors: a linked cancer-birth registry analysis. *Archives of Pediatrics and*
540 *Adolescent Medicine* **163**, 887-894.

541 **Choy JT & Brannigan RE** 2013 The determination of reproductive safety in men during and after
542 cancer treatment. *Fertility and Sterility* **100**, 1187-1191.

543 **Crow JF** (2000) The origins, patterns and implications of human spontaneous mutation. *Nature*
544 *Reviews Genetics* **1**, 40-47.

545 **De Iuliis GN, Thomson K., Mitchell LA, Finnie JM, Koppers AJ, Hedges A, Nixon B &**
546 **Aitken RJ** 2009 DNA damage in human spermatozoa is highly correlated with the efficiency of
547 chromatin remodeling and the formation of 8-hydroxy-2'-deoxyguanosine, a marker of oxidative
548 stress. *Biology of Reproduction* **81**, 517-524.

549 **Delbes G, Hales BF & Robaire B** 2007 Effects of the chemotherapy cocktail used to treat
550 testicular cancer on sperm chromatin integrity. *Journal of Andrology* **28**, 241-249.

551 **Dohle GR** 2010 Male infertility in cancer patients: Review of the literature. *International Journal of*
552 *Urology* **17**, 327-331.

553 **Evenson D & Jost L** 2000. Sperm chromatin structure assay is useful for fertility assessment.
554 *Methods in Cell Science* **22**, 169-189.

555 **Hales BF, Aguilar-Mahecha A & Robaire B** 2005 The stress response in gametes and embryos
556 after paternal chemical exposures. *Toxicology and Applied Pharmacology* **207**, 514-520.

557 **Hammoud SS, Nix DA, Zhang H, Purwar J, Carrell DT & Cairns BR** 2009 Distinctive
558 chromatin in human sperm packages genes for embryo development. *Nature* **460**, 473-478.

559 **Hill KA, Buettner VL, Halangoda A, Kunishige M, Moore SR, Longmate J, Scaringe WA**
560 **& Sommer SS** 2004 Spontaneous mutation in Big Blue® mice from fetus to old age: tissue-

561 specific time courses of mutation frequency but similar mutation types. *Environmental and Molecular*
562 *Mutagenesis* **43**,110-120.
563 **Huang VW, Lee CL, Lee YL, Lam KK, Ko JK, Yeung WS, Ho PC & Chiu PC.** 2015 Sperm
564 fucosyltransferase-5 mediates spermatozoa-oviductal epithelial cell interaction to protect human
565 spermatozoa from oxidative damage. *Molecular Human Reproduction* **21**, 516-526.
566 **Johnson SL, Dunleavy J, Gemmell NJ & Nakagawa S.** 2015 Consistent age-dependent declines
567 in human semen quality: a systematic review and meta-analysis. *Ageing Research Reviews* **19**, 22-33.
568 **Jónsson H, Sulem P, Kehr B, Kristmundsdottir S, Zink F, Hjartarson E, Hardarson MT,**
569 **Hjorleifsson KE, Eggertsson HP, Gudjonsson SA et al**. 2017 Parental influence on human
570 germline de novo mutations in 1,548 trios from Iceland. *Nature* 549:519-522.
571 **Kaarouch I, Bouamoud N, Madkour A, Louanjli , Saadani B3, Assou S, Aboulmaouahib**
572 **S, Amzazi S, Copin H, Benkhalifa M & Sefrioui O** 2018 Paternal age: negative impact on
573 sperm genome decays and IVF outcomes after 40 years. *Molecular Reproduction and Development*
574 **85**, 271-280.
575 **Kirkwood TB** 1977 Evolution of ageing. *Nature* **270**, 301–304.
576 **Kirkwood TBL & Austad AN** 2000 Why do we age? *Nature* **408**, 233-238.
577 **Kong A, Frigge ML, Masson G, Besenbacher S, Sulem P, Magnusson G, Gudjonsson SA,**
578 **Sigurdsson A, Jonasdottir A, Jonasdottir A et al.** 2012 Rate of de novo mutations and the
579 importance of father's age to disease risk. *Nature* **488**, 471-475.
580 **Koppers AJ, De Iuliis GN, Finnie JM, McLaughlin EA & Aitken RJ** 2008 Significance of
581 mitochondrial reactive oxygen species in the generation of oxidative stress in spermatozoa. *Journal*
582 *of Clinical Endocrinology and Metabolism* **93**, 3199-3207.
583 **Leonard B, Hart SN, Burns MB, Carpenter MA, Temiz NA, Rathore A, et al.** 2013
584 APOBEC3B upregulation and genomic mutation patterns in serous ovarian carcinoma.
585 *Cancer Research* **73**, 7222-7231.

586 **Looijenga LH, Gillis AJ, Stoop H, Biermann K & Oosterhuis JW** 2011 Dissecting the
587 molecular pathways of (testicular) germ cell tumour pathogenesis; from initiation to treatment-
588 resistance. *International Journal of Andrology* **34**, e234-251.
589 **Lyons DM & Lauring AS** 2017 Evidence for the selective basis of transition-to-transversion
590 substitution bias in two RNA viruses. *Molecular Biology and Evolution* **34**, 3205-3215.
591 **Manochantr S, Chiamchanya C & Sobhon P** 2012 Relationship between chromatin
592 condensation, DNA integrity and quality of ejaculated spermatozoa from infertile men. *Andrologia*
593 **44**, 187-199.
594 **Marcon L, Hale BF & Robaire** B 2008 Reversibility of the effects of subchronic exposure to the
595 cancer chemotherapeutics bleomycin, etoposide, and cisplatin on spermatogenesis, fertility, and
596 progeny outcome in the male rat. *Journal of Andrology* **29**, 408-417.
597 **Maselli J, Hales BF, Chan P & Robaire B** 2012 Exposure to bleomycin, etoposide, and cis-
598 platinum alters rat sperm chromatin integrity and sperm head protein profile. *Biology of*
599 *Reproduction* **86**, 166.
600 **Meeks JJ, Sheinfeld J & Eggener** SE 2012 Environmental toxicology of testicular cancer. *Urologic*
601 *Oncology* **30**, 212-215.
602 **Mortensen MS, Gundgaard MG & Daugaard G** 2011 Treatment options for carcinoma in situ
603 testis. *International Journal of Andrology* **34**, e32-36.
604 **Nili HA, Mozdarani H & Aleyasin A** 2009 Correlation of sperm DNA damage with protamine
605 deficiency in Iranian subfertile men. *Reproductive Biomedicine Online* **18**, 479-485.
606 **Nohmi T, Suzuki T & Masumura K** 2000 Recent advances in the protocols of transgenic mouse
607 mutation assays. *Mutation Research* **455**, 191-215.
608 **Pérez-Cerezales S, Miranda A & Gutiérrez-Adán A** 2012 Comparison of four methods to
609 evaluate sperm DNA integrity between mouse caput and cauda epididymidis. *Asian Journal of*
610 *Andrology* **14**, 335-337.
611 **R Core Team** 2004 R: a language and environment for statistical computing. R Foundation for
612 Statistical Computing, Vienna, Austria. http://www.R-project.org/

613 **Reuter VE** 2005 Origins and molecular biology of testicular germ cell tumors. *Modern Pathology*
614 *Supplement* **2**, S51-60.
615 **Sakkas D, Urner F, Bizzaro D, Manicardi G, Bianchi PG, Shoukir Y & Campana A** 1998
616 Sperm nuclear DNA damage and altered chromatin structure: effect on fertilization and embryo
617 development. *Human Reproduction Supplement* **4**, 11-19.
618 **Sawyer DE, Mercer BG, Wiklendt AM & Aitken RJ** 2003 Quantitative analysis of gene-specific
619 DNA damage in human spermatozoa. *Mutation Research* **529**, 21-34.
620 **Shelley MD, Burgon, K, Mason MD** 2002 Treatment of testicular germ-cell cancer: a cochrane
621 evidence-based systematic review. *Cancer Treatment Reviews* **28**, 237-253.
622 **Sherry ST, Ward MH, Kholodov M, Baker J, Phan L, Smigielski EM & Sirotkin K** 2001
623 dbSNP: the NCBI database of genetic variation. *Nucleic Acids Research* **29**, 308-311.
624 **Signorello LB, Mulvihill JJ, Green DM, Munro HM, Stovall M, Weathers RE, Mertens AC,**
625 **Whitton JA, Robison LL & Boice JD Jr** 2012 Congenital anomalies in the children of cancer
626 survivors: a report from the childhood cancer survivor study. *Journal of Clinical Oncology* **30**, 239-
627 245.
628 **Skakkebaek NE** 1972 Possible carcinoma-in-situ of the testis. *Lancet* **2**, 516-517.
629 **Stang A, Jansen L, Trabert B, Rusner C, Eberle A, Katalinic A, Emrich , Holleczek, B &**
630 **Brenner H** 2013 GEKID Cancer Survival Working Group. Survival after a diagnosis of testicular
631 germ cell cancers in Germany and the United States, 2002-2006: a high resolution study by
632 histology and age. *Cancer Epidemiology* **37**, 492-497.
633 **Ståhl O, Boyd HA, Giwercman A, Lindholm M, Jensen A, Kjær SK, Anderson H, Cavallin-**
634 **Ståhl E & Rylander** 2011 Risk of birth abnormalities in the offspring of men with a history of
635 cancer: a cohort study using Danish and Swedish national registries. *Journal of the National Cancer*
636 *Institute* **103**, 398-406.
637 **Sweeney C** 2001 History of testicular cancer chemotherapy: maximizing efficacy, minimizing toxicity.
638 *Seminars in Urologic Oncology* **19**, 170-179.
639 **van Basten JP, Schrafford Koops H, Sleijfer DT, Pras E, van Driel MF & Hoekstra HJ**

1997 Current concepts about testicular cancer. *European Journal of Surgical Oncology* **23**, 354-360.

Yatsenko AN & Turek PJ 2018 Reproductive genetics and the aging male. *Journal of Assisted Reproductionion and Genetics* [Epub ahead of print]

Zhan H, Jiang J, Sun Q, Ke A, Hu J, Hu Z, et al. 2017 Whole-exome sequencing-based mutational profiling of hepatitis B virus-related early-stage hepatocellular carcinoma. *Gastroenterology Research and Practice* **2017**, 2029315.

Ziglioli F, Maestroni U, Dinale F, Ciuffreda M & Cortellini P 2011 Carcinoma in situ (CIS) of the testis. *Acta Biomedica* **82**,162-169.

651 **Figure legends**

652 **Fig. 1.** Histological profile of the testes in BEP-exposed mice during the recovery phase in relation
653 to corresponding controls. Wk represents the numbers of weeks following a 3-week BEP exposure.
654 Images to the left are the controls, images to the right are BEP-exposed animals. Arrows indicate
655 seminiferous tubule sections exhibiting a severe disruption of spermatogenesis in association with
656 extensive vacuolization of the Sertoli cell cytoplasm.

657

658 **Fig. 2.** Analysis of BEP-exposed mice during the recovery phase. (A) Percentage of testicular cross
659 sections not revealing evidence of severely disrupted spermatogenesis, (B) testes weights, (C) mean
660 litter size and (D) number of embryonic resorptions at 14 dpc. Open bars are control treatments and
661 closed bars are chemotherapy-treated animals. Probability values inserted into the top right-hand
662 corner of each panel indicates the overall significance due to treatment according to ANOVA.
663 Asterisks at the head of the columns indicate the significance of the difference at each time point. *P
664 < 0.05; **P < 0.01; ***P < 0.001. At least 3 independent replicates per group.

665

666 **Fig. 3.** Sperm quality following exposure to BEP. (A) Number of spermatozoa recovered from the
667 caput epididymis, (B) number of spermatozoa recovered from the cauda epididymis, (C) percentage
668 of motile cells (D) percentage of progressively motile cells, (E) percentage of viable spermatozoa
669 exhibiting high levels of mitochondrial ROS generation by flow cytometry according to the probe
670 MitoSox Red (MSR). (F) percentage of viable spermatozoa exhibiting a high level of total cellular ROS
671 generation according to the probe dihydroethidium (DHE). Open bars are control treatments and
672 closed bars are chemotherapy treated animals. Probability values inserted into the top right-hand
673 corner of each panel indicates the overall significance due to treatment according to ANOVA.
674 Asterisks at the head of the columns indicate the significance of the difference at each time point. *P
675 < 0.05; **P < 0.01; ***P < 0.001. At least 3 independent replicates per group.

676

677 **Fig. 4.** Levels of DNA damage in the spermatozoa of mice recovering from BEP exposure as
678 measured by SCSA. Results of SCSA analysis for (A) caput epididymal spermatozoa and (B) cauda
679 epididymal spermatozoa. Open bars are control treatments and closed bars are chemotherapy-
680 treated animals. At least 3 independent replicates per group.
681
682 **Fig. 5** Impact of age on male reproduction in the Big Blue® mouse. (A) number of de novo mutations
683 in the whole-exome of embryos of pairs of young mice (1352 ± 20 mutations) and older mice (1357
684 ± 9 mutations), showed no statistical differences (Mann-Whitney U test, $P > 0.1$, n=4). (B) mutation
685 frequency in the whole-exome of embryos was not statistically different (Mann-Whitney U test, $P >$
686 0.1, n=4) between the offspring of young ($2.98 \times 10^{-7} \pm 4 \times 10^{-9}$ mutation/bp) and aged mice ($2.99 \times$
687 $10^{-7} \pm 2 \times 10^{-9}$ mutations/bp). Age dependent changes in: (C) testes weight; (D) sperm motility; (E)
688 DNA damage as measured by the SCSA assay; (F) flow cytometry analysis of percentage of cell
689 expressing abnormally high levels of 8OHdG formation; (G) mitochondrial superoxide generation in
690 caput and caudal epididymal spermatozoa; (H) mitochondrial membrane potential in caput and caudal
691 epididymal spermatozoa as measured by JC-1. Probability values inserted into the top right-hand
692 corner of each panel indicates the overall significance of differences due to the source of the
693 spermatozoa (caput or cauda epididymis). Asterisks at the head of the columns indicate the
694 significance of the difference at each time point. $^{*}P < 0.05$; $^{**}P < 0.01$; $^{***}P < 0.001$. At least 3
695 independent replicates per group.

Table 1 Mutation frequencies in the *cII* gene in testes of BEP-treated mice after 12 weeks recovery.

Group	N	Plaques screened	Mutant plaques	Mutant frequency[a] ($\times 10^{-5}$)	Mean mutant frequency ± SE ($\times 10^{-5}$)	Independent mutations	Mutation frequency[b] ($\times 10^{-5}$)	Mean mutation frequency ± SE ($\times 10^{-5}$)
Control	4	751667	7	0.9	1.4 ± 0.3	5	0.7	1.1 ± 0.2
		1070000	10	0.9		8	0.7	
		898333	16	1.8		11	1.2	
		770000	15	1.9		12	1.6	
BEP	4	257333	38	14.8	6.3 ± 2.9*	24	9.3	4.1 ± 1.8 *
		641667	27	4.2		22	3.4	
		443333	8	1.8		7	1.6	
		361667	16	4.3		7	1.9	

[a] Mutant frequency is the number of mutant plaques per total plaques screened ; [b] Mutation frequency is the number of independent mutations per total plaques screened; * $P \leq 0.05$;

Table 2 Spectra of independent mutations in the *cII* gene in testes of BEP-treated mice after 12 weeks recovery. Complex mutations are here defined as any combination of insertion, deletion or substitution found in a single mutant.

	Control		BEP	
Mutation	Number	%	Number	%
Transition				
G→A	16	44	13	22
C→T	5	14	9	15
A→G	1	3	2	3
T→C	0	0	2	3
Transversion				
G→C	0	0	2	3
G→T	5	14	5	8
C→G	1	3	0	0
C→A	1	3	4	7
A→C	1	3	2	3
A→T	0	0	3	5
T→G	0	0	1	2
T→A	0	0	3	5
Other				
Insertion	2	6	2	3
Deletion	4	11	9	15
Complex	0	0	3	5
Total	**36**	**100**	**60**	**100**

Table 3. Mutation frequencies in the *cII* gene in day 14 whole embryos produced from pairings between BEP-treated fathers and untreated mothers.

Group	N	Plaques screened	Mutant plaques	Mutant frequency[a] ($\times 10^{-5}$)	Mean mutant frequency ± SE ($\times 10^{-5}$)	Independent mutations	Mutation frequency[b] ($\times 10^{-5}$)	Mean mutation frequency ± SE ($\times 10^{-5}$)
Control	15[c]	330000	21	6.4	4.6 ± 0.4	13	3.9	2.9 ± 0.2
		355167	28	7.9		16	4.5	
		648333	28	4.3		19	2.9	
		455000	17	3.7		12	2.6	
		419667	22	5.2		17	4.1	
		578500	26	4.5		18	3.1	
		411833	21	5.1		19	4.6	
		358333	20	5.6		10	2.8	
		993333	48	4.8		21	2.1	
		540000	15	2.8		12	2.2	
		553333	20	3.6		16	2.9	
		661667	29	4.4		12	1.8	
		603333	17	2.8		13	2.2	
		768333	19	2.5		15	2.0	
		590000	31	5.3		12	2.0	
BEP	15[d]	383167	25	6.5	4.5 ± 0.6	14	3.7	2.7 ± 0.3
		489333	16	3.3		8	1.6	
		448333	37	8.3		20	4.5	
		638333	17	2.7		10	1.6	
		651667	15	2.3		5	0.8	
		355000	10	2.8		9	2.5	
		569333	41	7.2		25	4.4	
		718333	14	1.9		12	1.7	
		691667	36	5.2		23	3.3	
		505000	24	4.8		16	3.2	
		315000	8	2.5		7	2.2	
		376000	37	9.8		17	4.5	
		860000	35	4.1		20	2.3	
		561667	20	3.6		12	2.1	
		660000	21	3.2		14	2.1	

[a] Mutant frequency is the number of mutant plaques per total plaques screened; [b] Mutation frequency is the number of independent mutations per total plaques screened; [c] Two to four embryos from five pairings analysed; [d] Five embryos from three pairings analysed.

Table 4. Spectra of independent mutations in the *cII* gene in day 14 whole embryos produced from pairings between BEP-treated fathers and untreated mothers. Complex mutations are here defined as any combination of insertion, deletion or substitution found in a single mutant.

Mutation	Control		BEP	
	Number	%	Number	%
Transition				
G→A	70	31	67	32
C→T	42	19	22	10
A→G	2	1	9	4
T→C	11	5	10	5
Transversion				
G→C	9	4	11	5
G→T	23	10	29	14
C→G	2	1	5	2
C→A	15	7	7	3
A→C	2	1	4	2
A→T	5	2	2	1
T→G	2	1	10	5
T→A	7	3	3	1
Other				
Insertion	14	6	16	8
Deletion	19	8	16	8
Complex	2	1	2	1
Total	**225**	**100**	**213**	**100**

Table 5. Mutation frequencies in the *cII* gene in day 14 whole embryos produced from pairings between aged mice.

Group	N	Plaques screened	Mutant plaques	Mutant frequency[a] ($\times 10^{-5}$)	Mean mutant frequency ± SE ($\times 10^{-5}$)	Independent mutations	Mutation frequency[b] ($\times 10^{-5}$)	Mean mutation frequency ± SE ($\times 10^{-5}$)
Young Male x Young Female	5[c]	953333	18	1.9	3.5 ± 1.1	10	1.1	1.6 ± 0.1
		631667	14	2.2		11	1.7	
		576667	46	8.0		10	1.7	
		878333	27	3.1		15	1.7	
		575000	13	2.3		9	1.6	
Young Male x Old Female	5[d]	750000	13	1.7	1.9 ± 0.2	13	1.7	1.5 ± 0.1
		961667	23	2.4		16	1.7	
		701667	18	2.6		10	1.4	
		683333	12	1.8		10	1.5	
		471667	6	1.3		6	1.3	
Old Male x Young Female	5[e]	676667	18	2.7	2.4 ± 0.3	11	1.6	1.7 ± 0.1
		491667	15	3.1		9	1.8	
		481667	7	1.5		7	1.5	
		643333	19	3.0		14	2.2	
		638333	13	2.0		9	1.4	
Old Male x Old Female	7[f]	856667	26	3.0	3.0 ± 0.5	19	2.2	1.8 ± 0.2
		628333[g]	30	4.8		14	2.2	
		306667	12	3.9		7	2.3	
		385000	11	2.9		6	1.6	
		315000[g]	11	3.5		6	1.9	
		661667	10	1.5		7	1.0	
		446667	6	1.3		6	1.3	

[a] Mutant frequency is the number of mutant plaques per total plaques screened; [b] mutation frequency is the number of independent mutations per total plaques screened; [c]one to two embryos from each of four pairings analysed;[d] one embryo from each of five pairings analysed; [e] one embryo from each of five pairings analysed; [f] one to two embryos from each of five pairings analysed; [g] underdeveloped embryos.

Table 6 Mutation frequencies in the *cII* gene in livers from ageing mice

Age (months)	N	Plaques screened	Mutant plaques	Mutant frequency[a] ($\times 10^{-5}$)	Mean mutant frequency ± SE ($\times 10^{-5}$)	Independent mutations	Mutation frequency[b] ($\times 10^{-5}$)	Mean mutation frequency ± SE ($\times 10^{-5}$)
2-4	5	763333	29	3.8	3.3 ± 0.4	20	2.6	2.4 ± 0.3
		675000	26	3.9		22	3.3	
		766667	32	4.2		18	2.3	
		765000	17	2.2		13	1.7	
		755000	17	2.3		15	2.0	
9-11	5	490233	34	6.9	6.6 ± 0.5**	25	5.1	4.6 ± 0.3*
		557667	39	7.0		28	5.0	
		610667	50	8.2		31	5.1	
		501667	27	5.4		21	4.2	
		575000	33	5.7		20	3.5	
21-23	4	593333	53	8.9	6.8 ± 0.8**	35	5.9	4.4 ± 0.5*
		963333	56	5.8		36	3.7	
		558333	31	5.6		22	3.9	
		1325000	91	6.9		52	3.9	

[a] Mutant frequency is the number of mutant plaques per total plaques screened.

[b] Mutation frequency is the number of independent mutations per total plaques screened. $^{**}P < 0.01$; $^{*}P < 0.05$

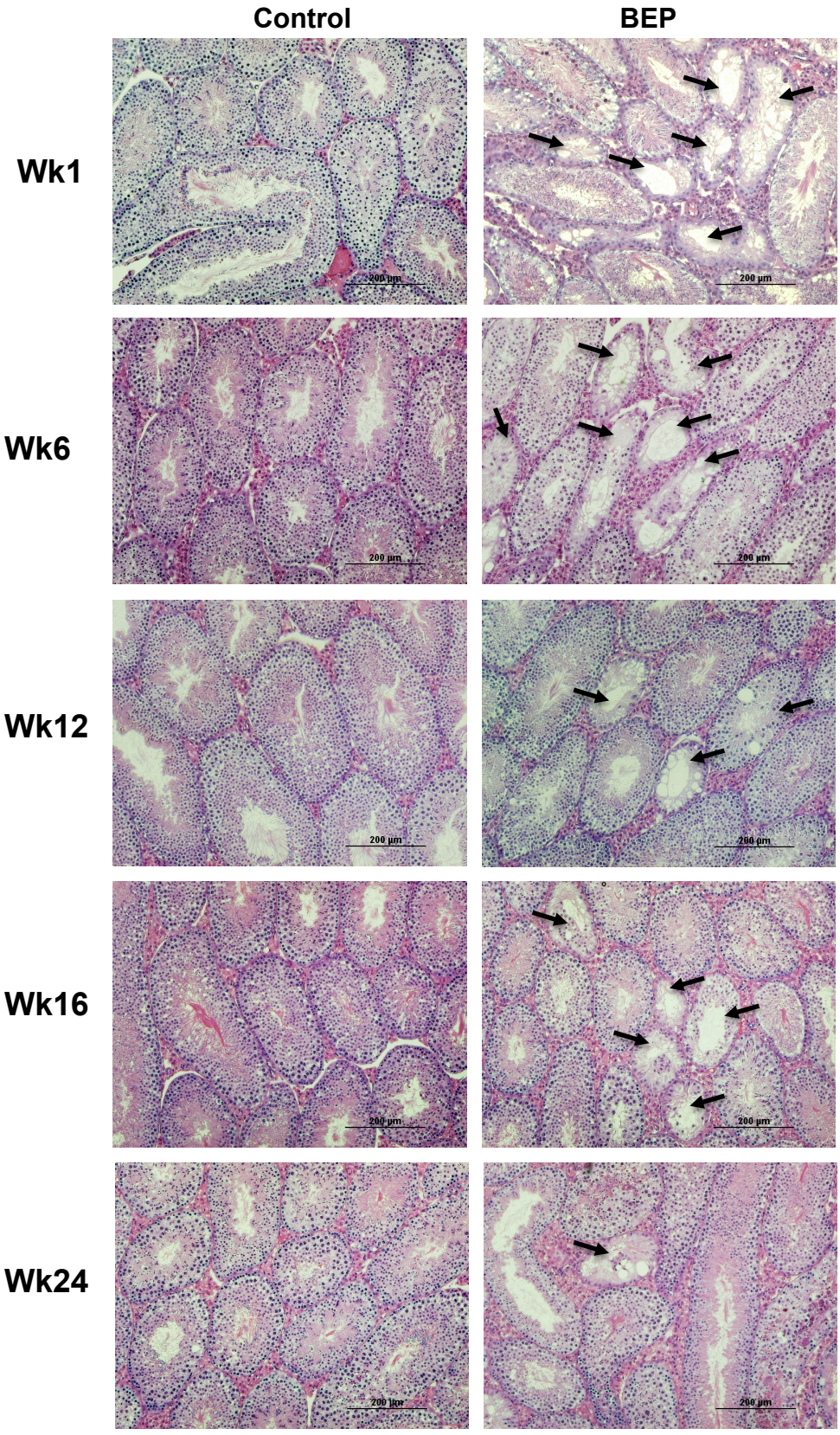
Control
BEP
Wk1
Wk6
Wk12
Wk16
Wk24
200 µm

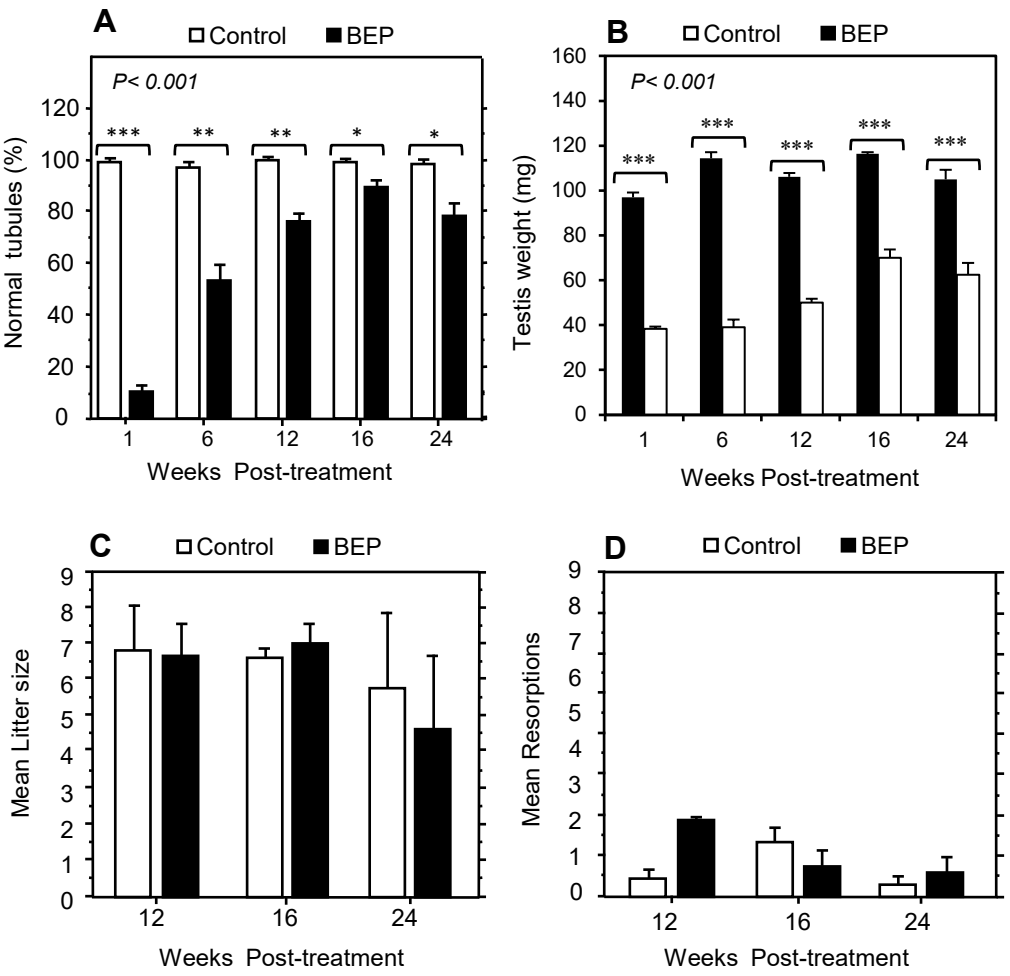
A
Control
BEP
P< 0.001
Normal tubules (%)
Weeks Post-treatment
B
Control
BEP
P< 0.001
Testis weight (mg)
Weeks Post-treatment
C
Control
BEP
Mean Litter size
Weeks Post-treatment
D
Control
BEP
Mean Resorptions
Weeks Post-treatment

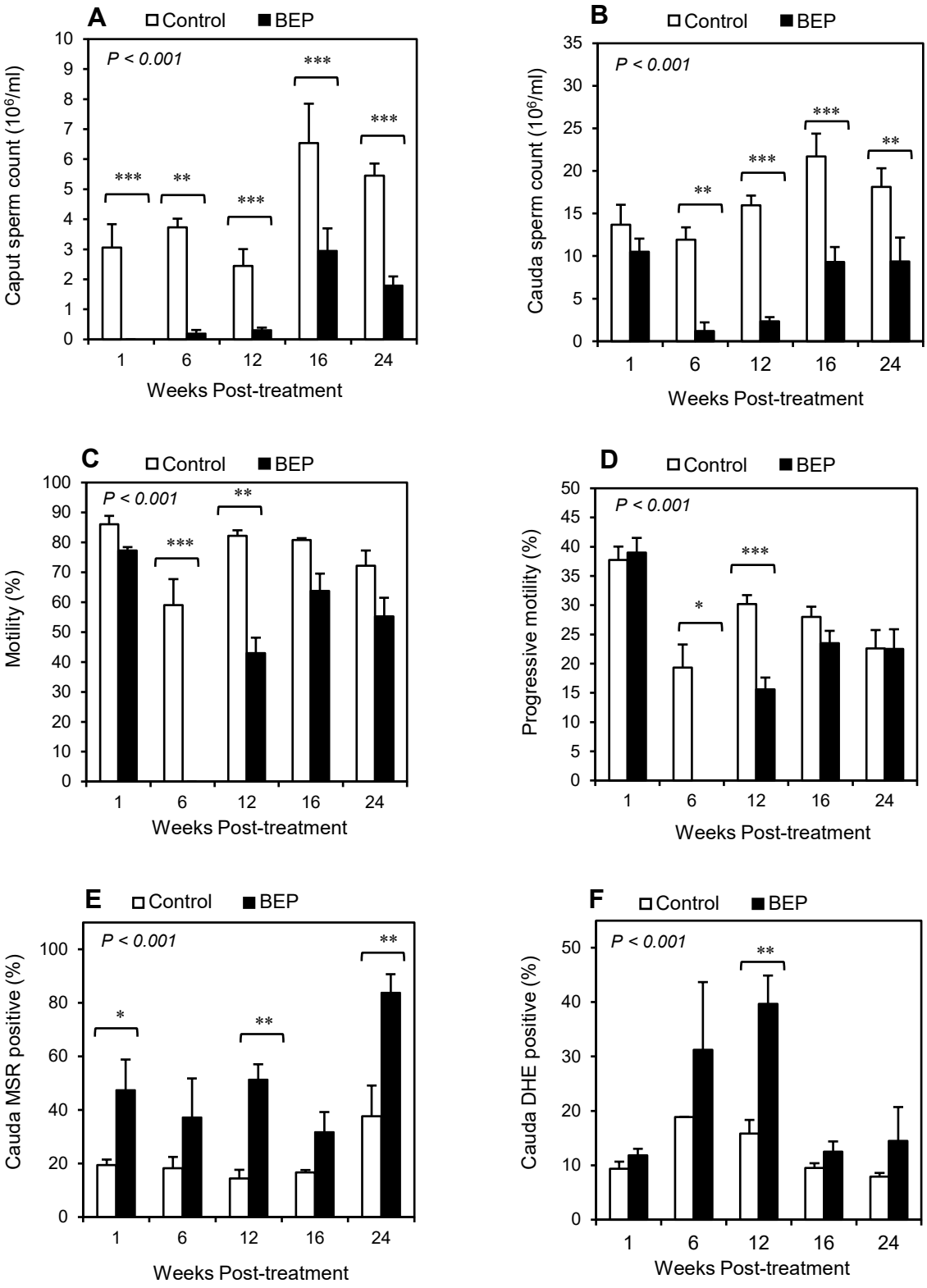
A
Control
BEP
P < 0.001
Caput sperm count (10⁶/ml)
Weeks Post-treatment
B
Cauda sperm count (10⁶/ml)
C
Motility (%)
D
Progressive motility (%)
E
Cauda MSR positive (%)
F
Cauda DHE positive (%)
1
6
12
16
24

Figure 4

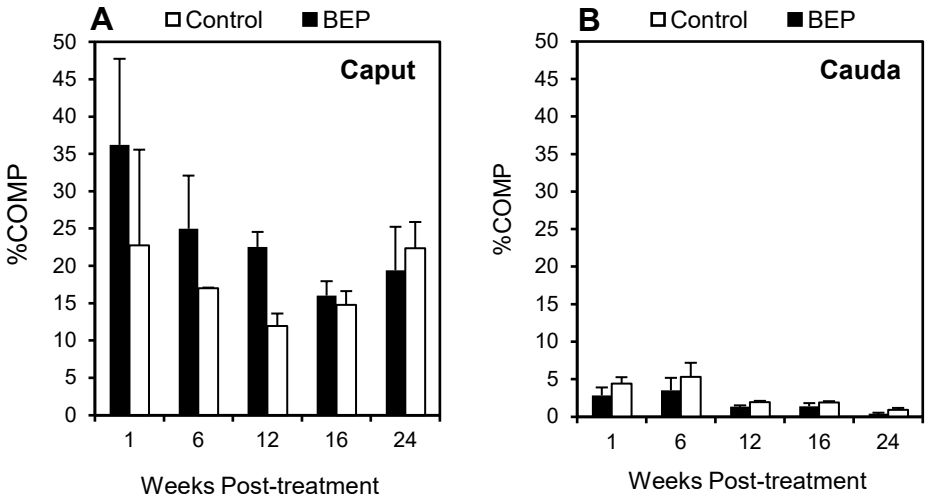
A
Control
BEP
Caput
%COMP
50
45
40
35
30
25
20
15
10
5
0
1
6
12
16
24
Weeks Post-treatment
B
Control
BEP
Cauda
%COMP
50
45
40
35
30
25
20
15
10
5
0
1
6
12
16
24
Weeks Post-treatment

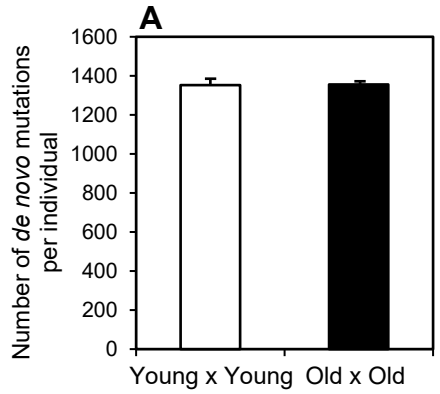
A
Number of de novo mutations per individual
1600
1400
1200
1000
800
600
400
200
0
Young x Young
Old x Old

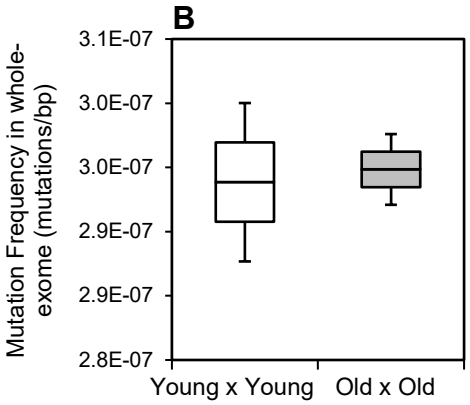
B
Mutation Frequency in whole-exome (mutations/bp)
3.1E-07
3.0E-07
3.0E-07
2.9E-07
2.9E-07
2.8E-07
Young x Young
Old x Old

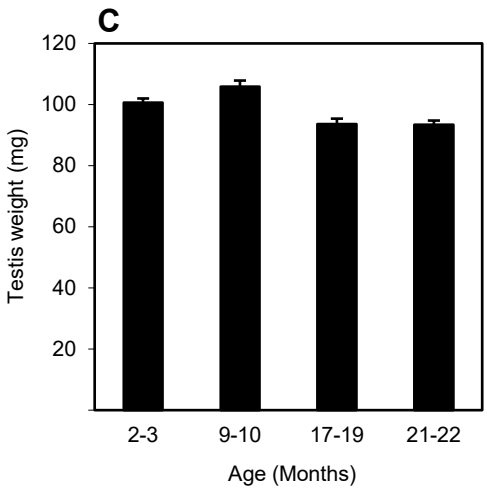
C
Testis weight (mg)
120
100
80
60
40
20
2-3
9-10
17-19
21-22
Age (Months)

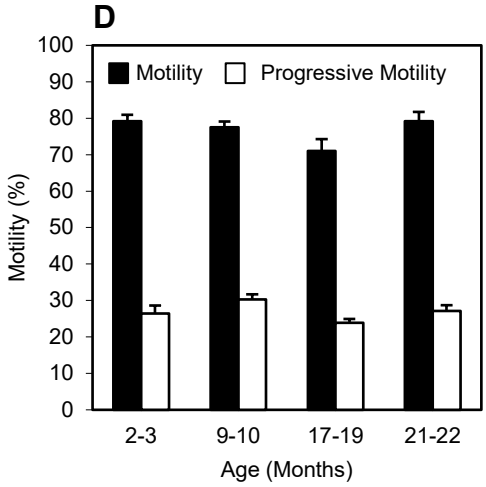
D
Motility
Progressive Motility
Motility (%)
100
90
80
70
60
50
40
30
20
10
0
2-3
9-10
17-19
21-22
Age (Months)

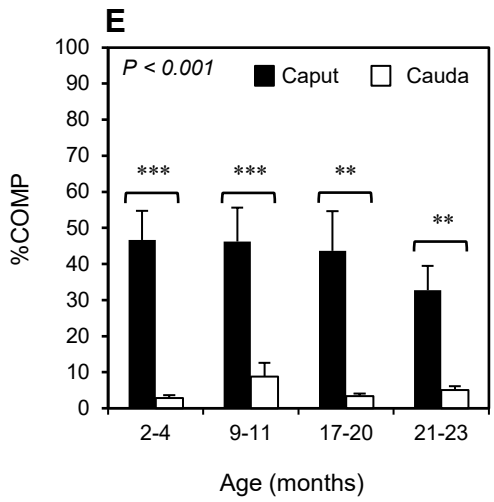
E
P < 0.001
Caput
Cauda
%COMP
***
***
**
**
2-4
9-11
17-20
21-23
Age (months)

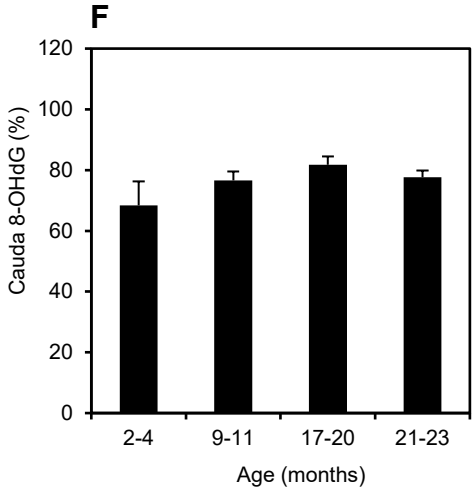
F
Cauda 8-OHdG (%)
120
100
80
60
40
20
0
2-4
9-11
17-20
21-23
Age (months)

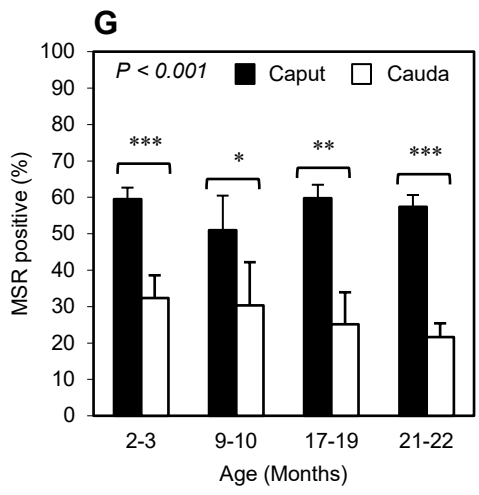
G
P < 0.001
Caput
Cauda
MSR positive (%)
***
*
**
***
2-3
9-10
17-19
21-22
Age (Months)

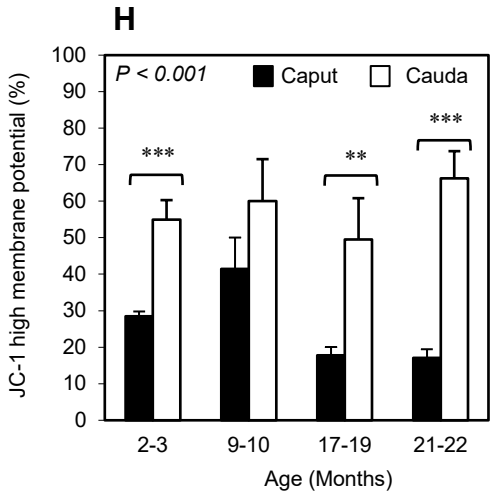
H
P < 0.001
Caput
Cauda
JC-1 high membrane potential (%)
***
**
***
2-3
9-10
17-19
21-22
Age (Months)